RADAR-DISDROMETER COMPARISON TO REVEAL ATTENUATION EFFECTS ON CASA RADAR DATA

Christopher Kerr[1,2], Guifu Zhang[3,4], and Petar Bukovcic[3,4]

[1]National Weather Center Research Experience for Undergraduates Program
and
[2]Clemson University, Clemson, South Carolina

[3]University of Oklahoma - School of Meteorology, Norman, Oklahoma

[4]University of Oklahoma – Atmospheric Radar Research Center, Norman, Oklahoma

ABSTRACT

X-band radar provides a high resolution image at the cost of significant attenuation. This is due to the X-band's short wavelength. In this study, a two-dimensional video disdrometer (2DVD) was deployed to the center of a triangle formed by three CASA dual-polarization X-band radars. The CASA radars provide measurements of reflectivity, differential reflectivity, specific differential phase, and co-polar cross-correlation coefficient of precipitation. Using drop size distributions obtained from the 2DVD, the radar variables are calculated and treated as the ground truth. The radar and disdrometer measurements are compared to reveal discrepancies. Biases and errors are calculated, and possible causes are investigated. These results can be used to further minimize the attenuation obstacle in X-band radar.

1. INTRODUCTION

A polarimetric radar transmits and receives horizontally and vertically polarized waves, allowing the size and shape of raindrops to be examined (Doviak and Zrnic, 1993; Bringi and Chandrasekar, 2001). Hence, polarimetric radar measurements allow the study of precipitation microphysics and improvement of quantitative precipitation estimation (Zhang et al. 2001). X-band radar produces fine resolution images and is most effective for low-level weather observations and short ranges (McLaughlin et al. 2009). The fine resolution measurements by X-band radar are achieved at the price of suffering severe attenuation. Hence, the radar measurements need to be corrected for this attenuation. It is important to have ground measurements made by the disdrometer to verify the radar measurements and the retrievals.

Figure 1: An OU disdrometer (2DVD)

Equipped with two high-speed cameras, the two-dimensional video disdrometer (2DVD) is able to measure the shape, size, and velocity of individual raindrops (Kruger and Krajewski 2002;

Corresponding author address: Christopher Kerr, 174 Murphey St., Barnwell, SC 29812
E-mail: cakerr@clemson.edu

Schönhuber et al. 2008), or, drop size distributions (DSDs). The measured DSDs can be used to calculate polarimetric radar variables that can service as ground-truth for verifying radar measurements.

From May 7-9, 2007, a series of rain events were measured by three CASA polarimetric X-band radars and a 2DVD operated by the University of Oklahoma. The three CASA radars used in this experiment are located southwest of the Oklahoma City area (Chickasha, Cyril, and Rush Springs, respectively) (Zhang et al. 2008). The disdrometer was deployed roughly near the center of the triangle formed by these three radars (KSAO, KCYR, and KRSP). From the data obtained by the disdrometer, the polarimetric radar variables reflectivity (horizontal polarization, Z_H), differential reflectivity (Z_{DR}), specific differential phase (K_{DP}), and co-polar cross correlation coefficient (ρ_{HV}) were calculated. The calculated radar variables are compared with the radar measurements. The error in each of the three radars can be evaluated quantitatively and qualitatively as related to attenuation. These results are presented in this paper.

2. METHODOLOGY

The initial step in analyzing the data is to identify the times of significant rainfall. Figure 2 is a plot of the rainfall rate (mm/hr) versus time on May 8, 2007, as determined by the 2DVD.

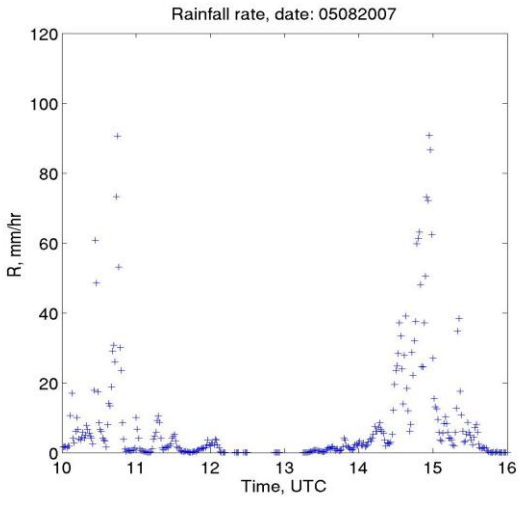

Figure 2: Rainfall rate versus time as determined by 2DVD

From this figure, the timeframe of precipitation is obvious. This is the timeframe in which the radar variables will be analyzed. The four radar variables (reflectivity, differential reflectivity, specific differential phase, and co-polar cross correlation coefficient) of each radar are averaged over 21 range gates and 3 rays above the location of the disdrometer to reduce the error. From the drop size distribution acquired from the 2DVD, reflectivity and differential reflectivity are calculated using the following equations:

$$Z_{hh,vv} = \frac{4\lambda^4}{\pi^4 |K_w|^2} \int_{D_{min}}^{D_{max}} \left| f_{hh,vv}(\pi, D) \right|^2 N(D)\, dD \quad (1)$$

$$Z_{DR} = 10 \log \frac{Z_{hh}}{Z_{vv}} \quad (2)$$

In these equations, *N(D)* is the DSD, *f(π,D)* is the backscattering amplitude, *λ* is the wavelength of the signal, and $K_w = (\varepsilon_r - 1) / (\varepsilon_r + 2)$, where ε_r is the complex dielectric constant of water (Bukovcic 2009).

Reflectivity is the most critical variable in this study. This is simply proportional to the backscattering of the radar pulse. Differential reflectivity is the ratio of the horizontal to vertical pulse return. A larger Z_{DR} means the raindrops are larger since raindrops become more oblate as they grow in size (Cao 2009). Specific differential phase is defined as the difference in propagation constants of the horizontal and vertical pulses. This variable is important in the fact that attenuation has no effect on the measurement (Zrnić and Ryzhkov 1996). The co-polar cross-correlation coefficient is a correlation of the horizontal and vertical returned signals. This variable is used to distinguish precipitation types within a storm, such as rain and hail (Cao 2009). Both raw radar data and attenuation corrected data were provided by CASA (Brotzge et al. 2006). The uncorrected and corrected variables are compared quantitatively and qualitatively. When comparing the radar and disdrometer data, low signal-to-noise (SNR) points were excluded by filtering those when reflectivity is less than 20 dBZ, and the rainfall rate is less than 1 mm/hr. Large differences between radar and disdrometer are investigated by visually inspecting the radar images. Figure 3 is an example of how visual inspection explains a large difference of an individual radar. In this case, KSAO's reflectivity

spiked while the remaining radars and 2DVD did not show a corresponding increase in reflectivity. The three images are roughly from 1102 UTC on May 8th.

(a)

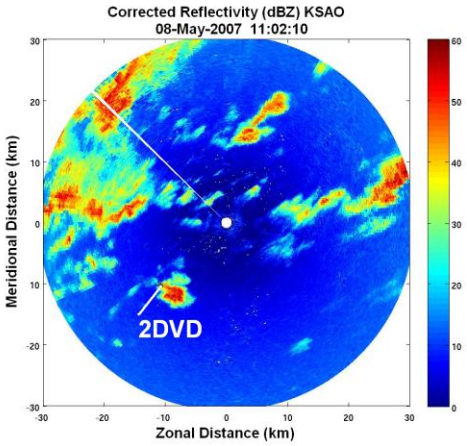

(b)

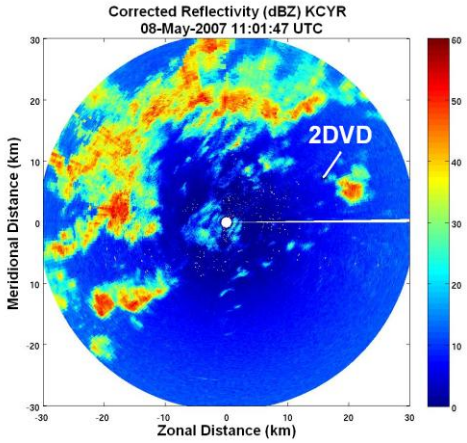

(c)

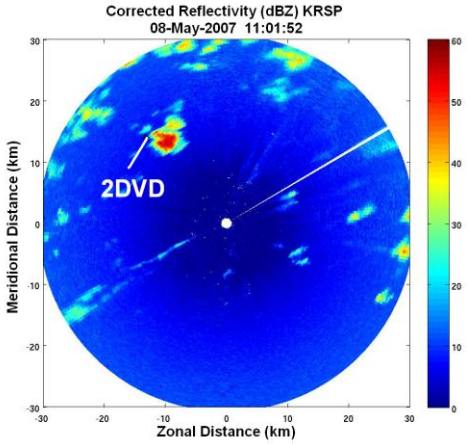

Figure 3: (a) KSAO, (b) KCYR, and (c) KRSP, CASA radar reflectivity at 1102 UTC on May 8th.

3. RESULTS

Polarimetric radar data sets were collected from May 7-9, 2007. Figure 4 (pg. 4-5) displays the plots of the four radar variables over time periods of rainfall for the three days. The plots contain data from the three radars as well as the 2DVD. Throughout the three days, differential reflectivity and co-polar cross-correlation coefficient were noisy.

Disdrometer determined reflectivity and differential reflectivity were calculated using drop size distributions. Figure 5 (pg. 5-6) displays the DSDs (along with radar estimations) from the three days. These retrievals include median volume diameter of the raindrops as well as the rainfall rate.

Comparing Figs. 4 and 5, the correspondence between the DSD retrievals and radar variables is clear. Differential reflectivity correlates with median volume diameter while rainfall rate correlates more so with reflectivity. The differences between the radar and disdrometer datasets were calculated for each variable on each day. They are quantified as mean bias and mean absolute difference as follows:

$$Bias = \frac{1}{N}\sum_{n=1}^{N}\left(Radar(n) - 2DVD(n)\right) \quad (3)$$

$$Abs\_Diff = \frac{1}{N}\sum_{n=1}^{N}\left|Radar(n) - 2DVD(n)\right| \quad (4)$$

In these equations, *n* is time while *Radar(n)* and *2DVD(n)* are the corresponding variable values.

Table 1 (pg. 7) displays the differences between the 2DVD data and the uncorrected radar variables while Table 2 (pg. 7) shows the differences between the 2DVD data and the corrected radar variables.

(a)

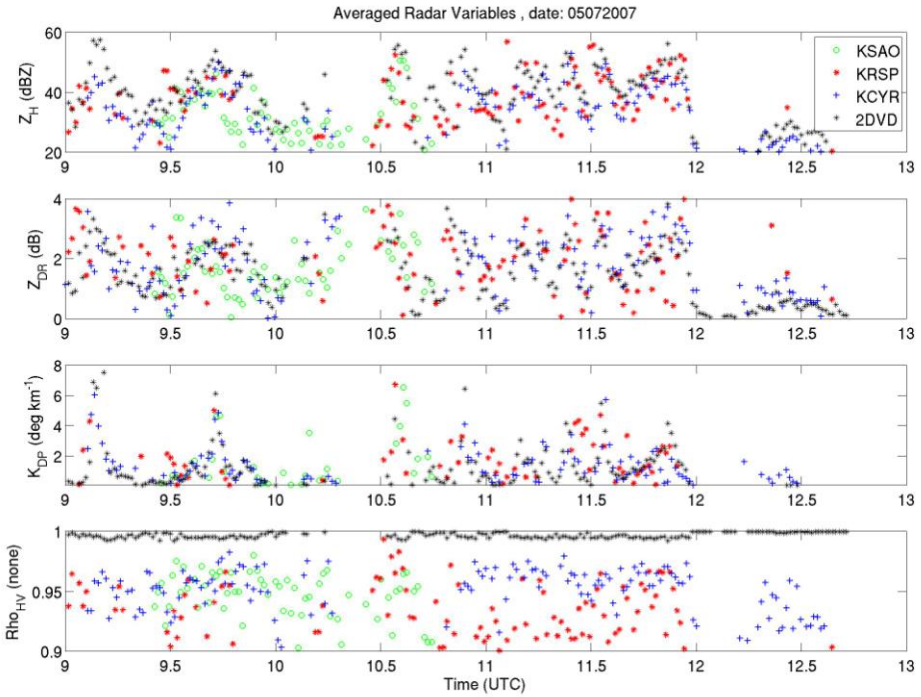
Averaged Radar Variables , date: 05072007
KSAO
KRSP
KCYR
2DVD
Z_H (dBZ)
Z_DR (dB)
K_DP (deg km^-1)
Rho_HV (none)
Time (UTC)

(b)

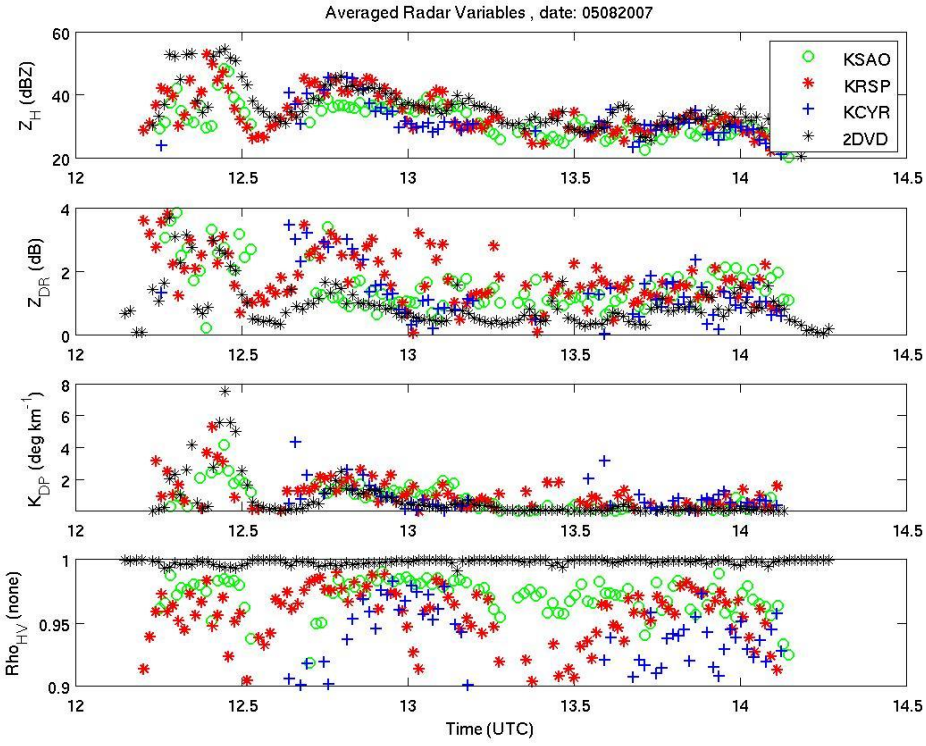
Averaged Radar Variables , date: 05082007
KSAO
KRSP
KCYR
2DVD
Z_H (dBZ)
Z_DR (dB)
K_DP (deg km^-1)
Rho_HV (none)
Time (UTC)

(c)

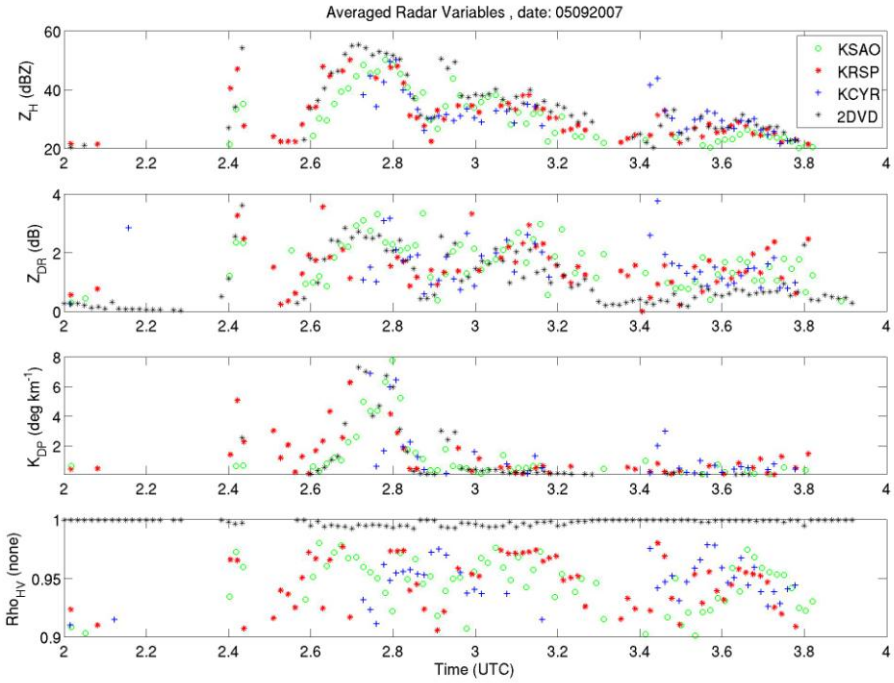

Figure 4: Plots of Z_H, Z_{DR}, K_{DP}, and ρ_{HV} as determined by radar and 2DVD on (a) May 7th, (b) May 8th, and (c) May 9th

(a)

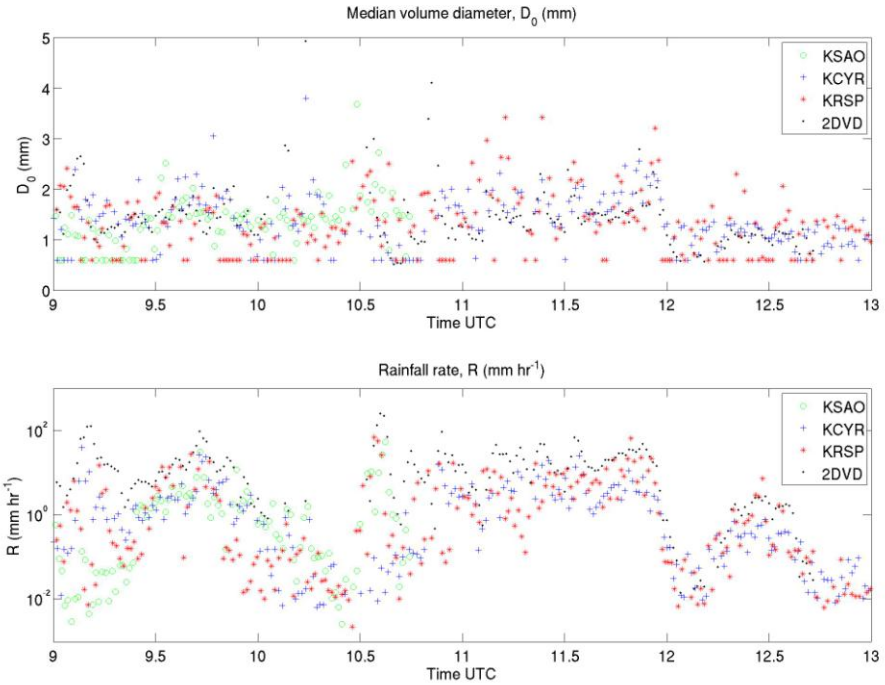

(b)

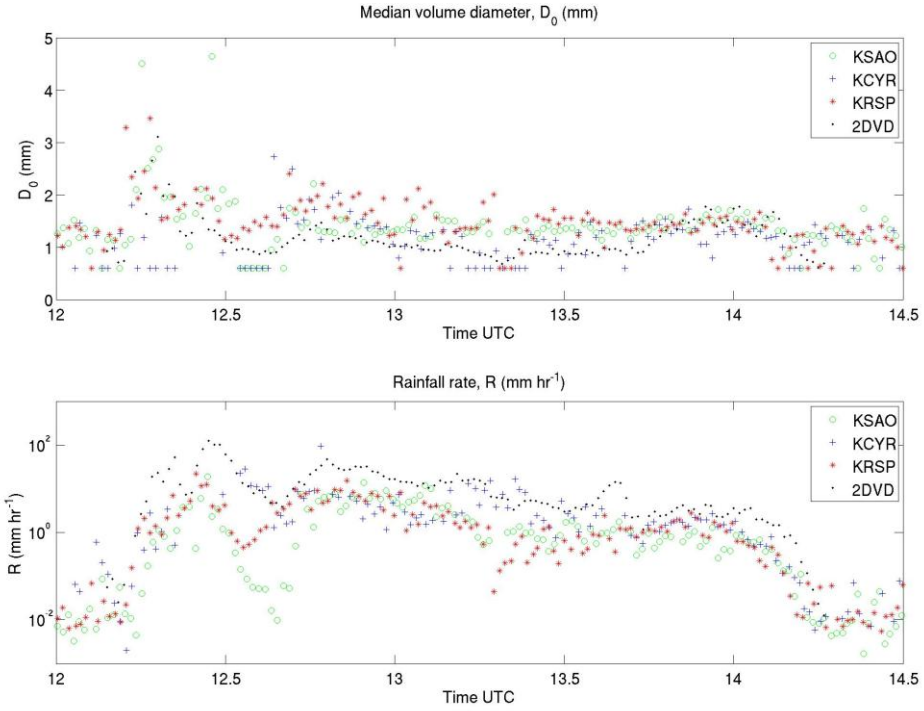

(c)

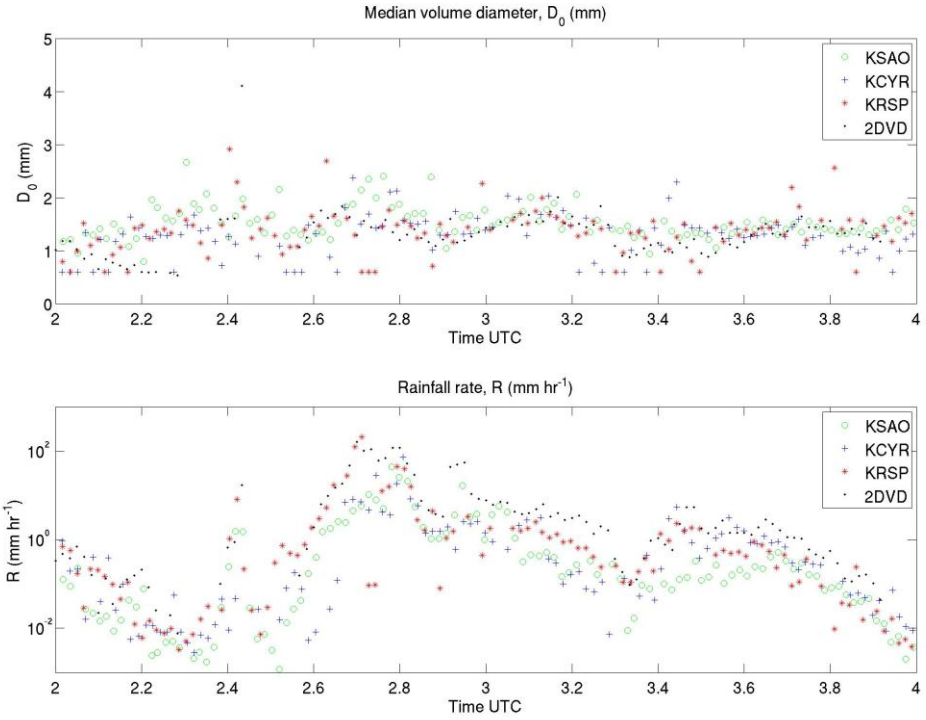

Figure 5: DSDs (median volume diameter and rainfall rate) for (a) May 7th, (b) May 8th, and (c) May 9th

Table 1: Bias and absolute difference between uncorrected radar measurements and calculations from disdrometer data. The largest differences among the radars are highlighted.

Error in Uncorrected Radar Variables										
		Zh (dBZ)			Zdr (dB)			Kdp (deg/km)		
		KSAO	KCYR	KRSP	KSAO	KCYR	KRSP	KSAO	KCYR	KRSP
7-May-07	Bias	-11.124	-11.424	-12.615	-1.407	-1.144	-1.920	-0.342	0.042	-0.014
	Abs. Diff.	11.650	11.502	12.967	1.487	1.244	2.084	1.645	0.904	1.321
8-May-07	Bias	-7.842	-6.842	-7.960	-0.110	-0.381	-0.561	-0.137	0.246	0.048
	Abs. Diff	7.876	6.940	8.127	0.432	0.445	0.758	0.562	0.387	0.809
9-May-07	Bias	-12.150	-7.502	-6.419	-1.000	-0.323	-0.249	-0.305	0.100	0.083
	Abs. Diff.	12.150	8.120	6.511	1.196	0.577	0.530	0.880	0.831	0.492

Table 2: Bias and absolute difference between corrected radar measurements and calculations from disdrometer data. The largest differences among the radars are highlighted.

Error in Corrected Radar Variables										
		Zh (dBZ)			Zdr (dB)			Kdp (deg/km)		
		KSAO	KCYR	KRSP	KSAO	KCYR	KRSP	KSAO	KCYR	KRSP
7-May-07	Bias	-6.0267	-5.7685	-3.4428	-0.1894	0.0680	0.3868	-0.3166	0.0430	-0.1038
	Abs. Diff.	7.7814	6.4426	5.7226	0.8230	0.6082	0.9994	1.6179	0.8631	1.3256
8-May-07	Bias	-4.4025	-3.6081	-2.5098	0.5544	0.3541	0.7559	-0.1279	0.2277	0.0960
	Abs. Diff.	4.7210	4.6475	4.7839	0.6334	0.5734	0.9580	0.5453	0.3885	0.7718
9-May-07	Bias	-5.5989	-3.8667	-3.3699	0.3251	0.3827	0.4077	-0.3142	0.1062	0.0887
	Abs. Diff.	6.0488	5.4332	4.2004	0.6239	0.7227	0.6860	0.8172	0.8135	0.4669

Throughout the three days, radar measured differential reflectivity was noisy. Figure 6 shows the differential reflectivity radar images from ~ 0930 UTC on May 7th. A noisy image is common when dealing with differential reflectivity due to ground clutter.

(a)

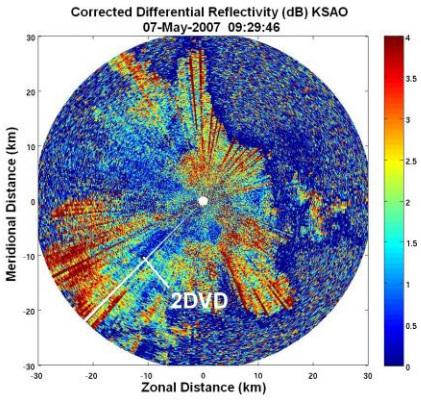

(b)

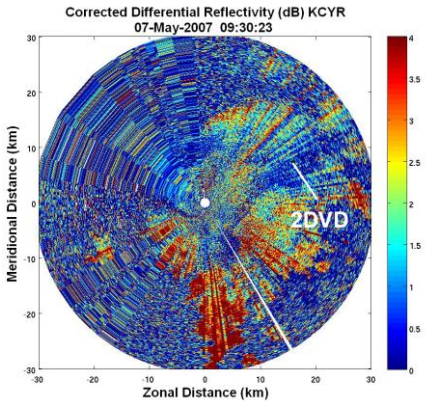

(c)

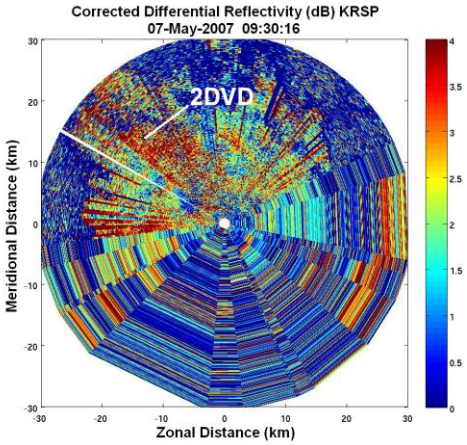

Figure 6: An example of noisy Z_{DR} measurement by (a) KSAO, (b) KCYR, and (c) KRSP

This explains why the plots (Figure 3) of Z_{DR} appear slightly chaotic. Although there seems to be disorder on the radar images, the error in differential reflectivity is not absurd. The co-polar cross-correlation coefficient error is high since this variable usually has a range of only 0.1 for all types of precipitation.

3.1. MAY 07, 2007

The radar with the largest error in reflectivity was the KSAO radar. This may be the result of the fact that the radar went offline at approximately 1045 UTC. Because of this, there are fewer data points. Prior to 0930 UTC, heavy precipitation over the KSAO radar completely dampened the signal before the pulse was able to reach the 2DVD site. The line of rain also passed over the KRSP radar, weakening the signal. The reflectivity plot in Figure 3 shows a large difference between the radar and disdrometer reflectivity before and after 1000 UTC. The 2DVD suggests that the reflectivity over the site should have been slightly less than 50 dBZ. Figure 7 shows the three radar images at approximately 1015 UTC.

(a)

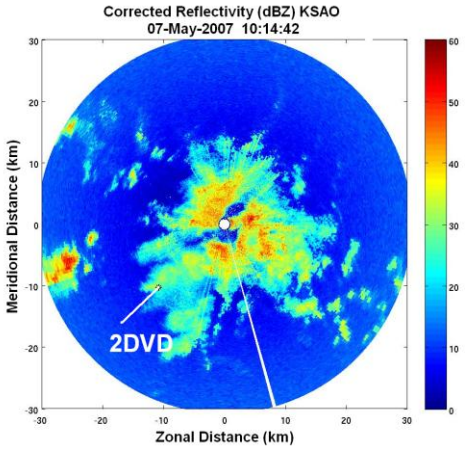

(b)

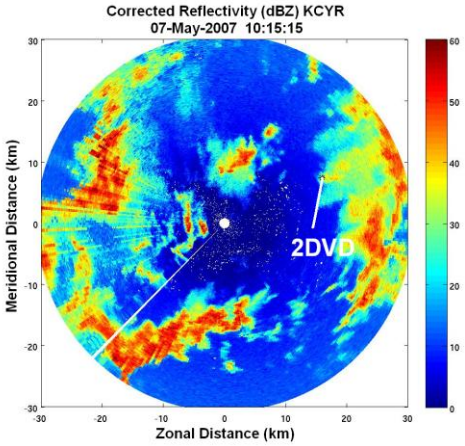

(c)

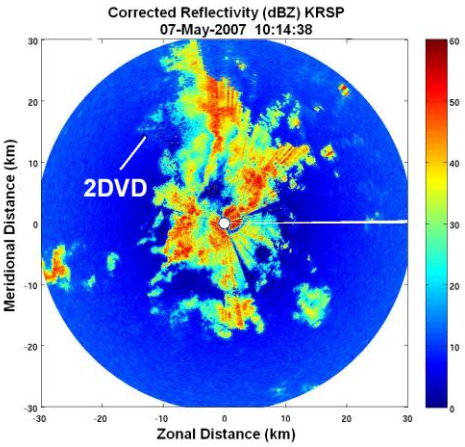

Figure 7: Reflectivity images measured at 1015 UTC on May 7, 2007 by (a) KSAO, (b) KCYR, and (c) KRSP.

Table 3 below displays the bias and absolute difference between the radars and 2DVD from 1000 to 1030 UTC.

Table 3: Reflectivity error between 1000 and 1030 UTC on May 7th

	KSAO	KCYR	KRSP
Bias	-8.4654	-4.1183	NaN
Abs. Diff.	8.4654	4.1183	NaN

The large error in KSAO's reflectivity reading during this time span had a significant effect on the day's average bias and absolute difference. KRSP reflectivity was undefined during this time because all reflectivity readings, if any, were below 20 dBZ.

3.2. MAY 08, 2007

In terms of reflectivity, KSAO differed the most from the disdrometer. Upon examination, the largest error in KSAO's reflectivity seems to fall between 1230 and 1300 UTC. Figure 8 shows the radar images at approximately 1245 UTC.

(a)

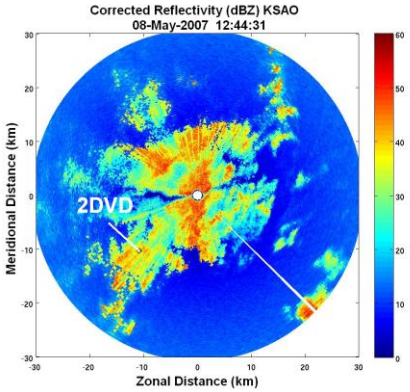

(b)

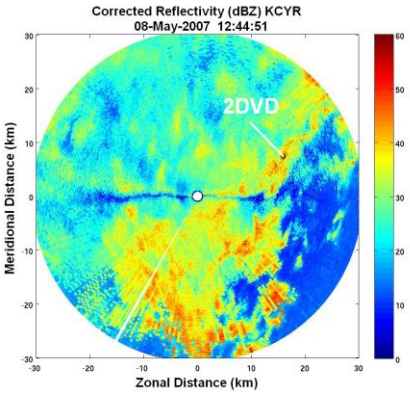

(c)

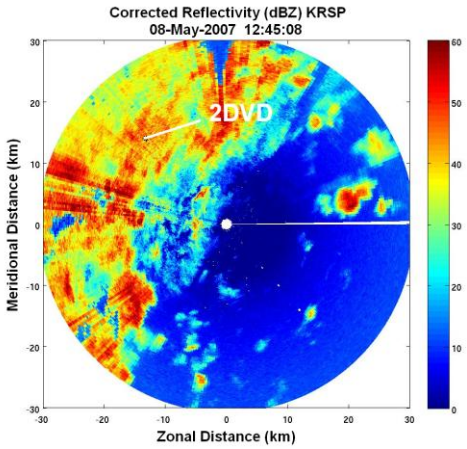

Figure 8: Reflectivity images measured at 1245 UTC on May 8, 2007 by (a) KSAO, (b) KCYR, and (c) KRSP

Table 4: Reflectivity error between 1230 and 1300 UTC May 8th.

	KSAO	KCYR	KRSP
Bias	-5.4673	-2.3705	-0.6723
Abs. Diff.	5.4673	4.0920	3.7941

From these three radar images, the source of the error seems to originate from the rain mass over the KSAO radar. Because this heavy precipitation was directly over the radar, the signal attenuated very rapidly. The same problem was present for the KCYR radar. Using the KRSP image, the heavy precipitation area is more evident. The precipitation was not directly over KRSP, which allowed the radar to obtain a more accurate reflectivity reading over the 2DVD site. The differential reflectivity reading was also affected by attenuation. KRSP had a significantly large difference in differential reflectivity from ~ 1230 to 1330 UTC. Table 5 below displays the average difference between the 2DVD and the radars during this timeframe.

Table 5: Differential reflectivity error between 1230 and 1330 UTC May 8th

	KSAO	KCYR	KRSP
Bias	0.4529	0.5623	1.0062
Abs. Diff.	0.5453	0.7219	1.0778

For all three radars, differential reflectivity appears to have been overcorrected. In terms of specific differential phase, there is no radar that had a significantly greater error than any other. In

regards to this variable, the elevation difference (between radar and 2DVD measurements) played the most significant role in these variations.

3.3. MAY 09, 2007

The largest error in reflectivity was once again in the KSAO radar. Figure 3 shows the KSAO reflectivity readings were low relative to the 2DVD estimation roughly between 0240 and 0320 UTC. The biases and absolute differences during this time span are presented in Table 6.

Table 6: Reflectivity error between 0240 and 0320 UTC, May 9th

	KSAO	KCYR	KRSP
Bias	-4.6063	-7.2301	-4.1987
Abs. Diff.	5.3174	7.2301	4.5757

Inspection of the radar images shows a rain band between the 2DVD site and KSAO. This means KSAO's signal was weakened by attenuation. There was also a mass of heavy precipitation between the 2DVD and KCYR radar. This accounts for the large difference during this time frame. The sudden KCYR spike in reflectivity, differential reflectivity, and specific differential phase slightly after 0324 UTC is due to a disagreement in storm position amongst the three radars. KSAO and KRSP show the cell swiping the 2DVD site while KCYR shows the cell directly over this location. An example of this problem is presented in the methodology section.

4. CONCLUSIONS

Although an attenuation correction was originally applied, the modification did not completely eliminate the error in the radar measurements. In some cases, the error was only reduced by fifty percent while other variables were overcorrected. Some variables had relatively large errors mainly due to severe attenuation. This was induced by heavy precipitation directly over the radar site or between the 2DVD site and radar. On all three days, KSAO had the greatest error in reflectivity among the three radars. The reason ranges from attenuation to loss of power. The leading cause of significant error within a day was a large difference in a short time frame. These time frames were analyzed. Differential reflectivity's error may originate from model error, miss-calibration, differential attenuation effects, and the difference in DSD between the elevation at which the radar attained measurements and ground level, where the 2DVD collected readings. KRSP was located farthest from the 2DVD site which resulted in this radar having the largest bias in differential reflectivity throughout the three days. The minor discrepancies in specific differential phase measurements support the theory that only attenuation was the cause of major error in reflectivity since K_{DP} is not affected by this problem. As seen in Figure 3, differential reflectivity and co-polar cross-correlation coefficient were very noisy. In terms of co-polar cross-correlation coefficient, system error is at fault rather than a physical problem such as attenuation. The noisiness of differential reflectivity was most likely caused by ground clutter. The error in this variable is not significant enough to draw conclusions pertaining to attenuation. The results from this study can potentially be used for further attenuation correction.

5. ACKNOWLEDGMENTS

The authors would like to thank Ben Root and Tim Bonin for programming assistance during this study. This material is based upon work supported by the National Science Foundation under Grant No. ATM-0648566 and ATM-0608168. The statements, findings, conclusions, and recommendations are those of the authors and do not necessarily reflect the views of the National Science Foundation.

6. REFERENCES

Brandes, E. A., G. Zhang, and J. Vivekanandan, 2004: Drop size distribution retrieval with polarimetric radar: model and application. *J. Appl. Meteor.,* **43**, 461-475

Bringi, V.N. and V. Chandrasekar, 2001: *Polarimetric Doppler Weather Radar: Principles and applications*. Cambridge University Press. 648 pp.

Brotzge, J., K. Droegemeier, and D. McLaughlin, 2006: Collaborative Adaptive Sensing of the Atmosphere (CASA): New radar system for improving analysis and forecasting of surface weather conditions. *Journal Transportation Research Board*, **1948**,145-151.

Bukovcic, Petar, Dusan Zrnic, Guifu Zhang, and Qing Cao, 2009: A Study of Precipitation Microphysics Using S- and X-Band Polarimetric Radar and Disdrometer Measurements.

Bukovcic, Petar, 2009: A Study of Precipitation Microphysics Using Polarimetric Radar and Disdrometer Measurements. M.S. thesis, School of Meteorology, University of Oklahoma, 112 pp.

Cao, Q., 2009: Observational study of rain microphysics and rain retrieval using polarimetric radar data. PhD dissertation, University of Oklahoma, 208 pp.

Cao, Qing, Guifu Zhang, Edward Brandes, Terry Schuur, Alexander Ryzhkov, Kyoko Ikeda, 2008: Analysis of Video Disdrometer and Polarimetric Radar Data to Characterize Rain Microphysics in Oklahoma. Journal of Applied Meteorology and Climatology, 47, 2238-2255

Chandrasekar, V., D. J. McLaughlin, J. A. Brotzge, M. Zink, B. D. Phillips, and Y. Wang, 2008: Distributed collaborative adaptive radar network: The CASA IP-1 testbed observations *Symp. Recent Develop. Atmos. Applications Radar Lidar* New Orleans, LA, Amer. Meteor. Soc., 5.4.

Doviak, R. J., and D. S. Zrnic, 1993: Doppler Radar and Weather Observations. Academic Press, San Diego, Calif.

Kruger, A., and W. F. Krajewski, 2002: Two-Dimensional Video Disdrometer: A Description. *J. Atmos. Oce. Tech.,* **19**, 602-617

McLaughlin, D., D. Pepyne, V. Chandrasekar, B. Philips, J. Kurose, M. Zink, K. Droegemeier, S. Cruz-Pol, F. Junyent, J. Brotzge, D. Westbrook, N. Bharadwaj, Y. Wang, E. Lyons, K. Hondl, Y. Liu, E. Knapp, M. Xue, A. Hopf, K. Kloesel, A. Defonzo, P. Kollias, K. Brewster, R. Contreras, B. Dolan, T. Djaferis, E. Insanic, S. Frasier, and F. Carr, 2009: Short-Wavelength Technology and the Potential for Distributed Networks of Small Radar Systems. *Bulletin of the American Meteorological Society*, **90**, 1797–1817.

Schönhuber, M., G. Lammer, W.L. Randeu, 2008: The 2D-Video-Distrometer. *Precipitation: Advances in Measurement, Estimation and Prediction*. Springer. pp. 3-31.

Zhang, G., J. Vivekanandan, and E. Brandes, 2001: A method for estimating rain rate and drop size distribution from polarimetric radar. *IEEE Trans. Geosci. Remote Sensing,* vol. **39**, No.4, 830-840.

Zhang, G., Q. Cao, M. Xue, P. Chilson, M. Morris, R. Palmer, J. Brotzge, T. Schuur, E. Brandes, K. Iketa, A. Ryzhkov, D. Zrnic, and E. Jessup , “A Field Experiment to Study Rain Microphysics Using Video Disdrometers, A Profiler, and Polarimetric S and X-Band Radars,” Symposium on Recent Developments in Atmospheric Applications of Radar and Lidar, AMS Annual Meeting, New Orleans, LA, January, 2008

Zrnić, D. S., A. Ryzhkov, 1996: Advantages of Rain Measurements Using Specific Differential Phase. Journal of Atmospheric and Oceanic Technology, 13, 454-464